Characterization of N n = 2 − 18 + clusters produced by 252Cf fission fragment impact on a N 2 ice target

ARTICLE *in* CHEMICAL PHYSICS · NOVEMBER 2007

Impact Factor: 1.65 · DOI: 10.1016/j.chemphys.2007.08.022

6 AUTHORS, INCLUDING:

Francisco Fernandez-Lima
Florida International University
66 PUBLICATIONS **502** CITATIONS
SEE PROFILE

Enio Frota da Silveira
Pontifícia Universidade Católica do Rio de …
179 PUBLICATIONS **1,173** CITATIONS
SEE PROFILE

Marco Nascimento
Federal University of Rio de Janeiro
143 PUBLICATIONS **1,912** CITATIONS
SEE PROFILE

Available online at www.sciencedirect.com
ScienceDirect
Chemical Physics 340 (2007) 127–133
Chemical Physics
www.elsevier.com/locate/chemphys

Characterization of $N^+_{n=2-18}$ clusters produced by ^{252}Cf fission fragment impact on a N_2 ice target

F.A. Fernández-Lima [a,b], C.R. Ponciano [a], G.S. Faraudo [a], M. Grivet [c], E.F. da Silveira [a], M.A. Chaer Nascimento [d,*]

[a] Departamento de Física, Pontifícia Universidade Católica, Rio de Janeiro, Brazil
[b] Instituto Superior de Tecnologías y Ciencias Aplicadas, Cuba
[c] CETUC, Pontifícia Universidade Católica, Rio de Janeiro, Brazil
[d] Instituto de Química, Universidade Federal do Rio de Janeiro, Rio de Janeiro, Brazil

Received 23 October 2006; accepted 15 August 2007
Available online 31 August 2007

Abstract

The structures and abundances of $N^+_{n=2-18}$ clusters produced by impact of ^{252}Cf fission fragments (FF) on N_2 ice target are analyzed. A systematic search for the more stable conformers at the DFT/B3LYP level and a recently proposed methodology for a proper taxonomic description (*D*-plot) of the cluster isomers in series are presented. Several new members of the previously reported linear series have been identified. Besides that, three new series of clusters and some other stable structures have also been found. The clusters stability and ionization potential analysis showed that the ^{252}Cf FF exponential dependence of the cluster yield with its mass is rather a consequence of the production mechanism than that of the cluster structure.

Keywords: Nitrogen clusters; Density functional theory; Cluster stability; Cluster taxonomy; Binding energy; ^{252}Cf-PDMS

1. Introduction

The generation of ion clusters from several condensed gases has been recently studied by ~60 MeV ^{252}Cf fission fragment (FF) impact on ice surfaces at controlled temperature [1–7]. Processes in which very fast and highly charged projectiles induce electronic sputtering on low-temperature condensed-gas solids (ices) are relevant since they occur in cometary's surfaces and outer-solar-system bodies [7–12]. When the target is a frozen gas with low molecular weight such as nitrogen, one might expect that the desorbed species would be mostly atoms or small molecules with small number of constituents because these gases condensate only through weak van der Waals interactions. However, the emission of a large number of cluster ions N^+_n has been observed in experiments with ^{252}Cf FF (*n* up to ~22) [7], with keV He^+ ion bombardment (*n* up to ~30) [8] and with 1.5 MeV/u Ar^{13+} ion impact (*n* up to ~20) [11].

Since many of the clusters' characteristics (e.g. geometry, binding energy) are difficult to obtain directly from experiment, theoretical models and computational methods are very useful in predicting them and therefore helping the interpretation of the spectroscopic and mass spectrometric data. Predictive *ab initio* theoretical chemistry is essential for characterizing the structure of weak-linked species. Nitrogen clusters have been characterized by *ab initio* methods such as the Hartree–Fock [13–19], the Moller–Plesset (MP) perturbation theory [14–18,20–23] and the coupled cluster method (CC) [24], as well as by density functional theory (DFT) [14,15,17,21,23,25,26]. Although studies on small ionic nitrogen clusters N^+_n have been recently reported for $n = 3$ [18,19,23], $n = 4$ [13b], $n = 5$ [18,19,23,26], $n = 7$ [22] and $n = 11$ [17], a systematic and

* Corresponding author. Tel.: +55 21 2562 7563; fax: +55 21 2562 7265.
E-mail address: chaer@iq.ufrj.br (M.A.C. Nascimento).

0301-0104/$ - see front matter © 2007 Elsevier B.V. All rights reserved.
doi:10.1016/j.chemphys.2007.08.022

accurate theoretical calculation of nitrogen ionic clusters, to the best of our knowledge, has not yet been performed.

In this paper, the population distribution of positively charged nitrogen clusters, N_n^+, for n up to 22, generated by ^{252}Cf FF impact on a N_2 condensed target is examined. A systematic search for the possible conformers of the N_n^+ clusters (for n up to 18) has been conducted using DFT at the B3LYP/6-311G** level and a taxonomic study of the obtained theoretical structures is described. The results of these calculations are used to investigate if the mass spectra population distribution can be understood in terms of the clusters stability and the ionization potential.

2. Experimental method

The experimental features of ^{252}Cf-PDMS can be found elsewhere [1,5,7,27]. Briefly, an N_2 ice target was grown by condensation of N_2 gas over an Au substrate at controlled low temperature (in the 30–40 K range). A fission fragment produced by a ^{252}Cf source eventually collides with the N_2 ice target inducing ion desorption in high vacuum conditions (in the low 10^{-8} mbar). The desorbed ions are accelerated by an extraction field towards the drift region and are detected by a micro channel plate detector. The mass analysis is performed by the time-of-flight technique (TOF) [27].

3. Computational details

Positively charged nitrogen cluster structures were calculated using DFT at the B3LYP/6-311G** level with the Jaguar 6.0 software [28]. The basis set superposition error (BSSE) was found to be of the order of 0.02 eV. The accuracy of the B3LYP functional is known to be of the order of ~3 kcal/mol, meaning that conformers differing by less than that amount cannot be distinguished at this level of calculation. No symmetry restrictions have been imposed in the process of geometry optimization. A vibrational analysis was performed in order to verify that the optimized structures correspond to real minima in the potential energy surfaces. It is true that some of the N_n^+ clusters may exhibit low lying electronic excited states. However, the usual life-times of these excited states are much shorter than the time of scale of the TOF experiments, which is of the order of 10^{-6} s. Thus, it is quite reasonable to assume that the detected ions are all in their ground electronic states.

4. Results and discussion

4.1. N_n^+ optimized structures

A systematic search for all the possible N_n^+ structures has been performed and their total internal energies (including the zero-point correction) are presented in Table 1. The obtained structures (see Fig. 1) can be classified in four series by their conformational similarities (as described below) or by their total internal energy (*D*-plot section).

Table 1
The N_n^+ internal energy (including ZPE) at the B3LYP/6-311G** level of calculation

Cluster	Energy (eV)	Cluster	Energy (eV)	Cluster	Energy (eV)
N^+	−1468.38	N_6^+ I	−8926.80	N_9^+ I	−13395.39
N^0	−1482.85	N_6^+ B	−8926.35	N_9^+ III	−13398.77
N_2^+	−2965.20	N_6^+ A	−8917.36	N_{10}^+ I	−14884.28
N_2^0	−2981.04	N_{6a}^+ IV	−8924.77	N_{10}^+ II	−14875.73
N_3^+ B	−4454.70	N_{6b}^+ IV	−8924.75	N_{11}^+ I	−16373.66
N_3^0 I	−4467.27	N_{7a}^+ C	−10419.02	N_{12}^+ I	−17862.92
N_3^+ III	−4454.96	N_{7b}^+ C	−10418.98	N_{12}^+ II	−17852.84
N_3^0 III	−4465.72	N_7^+ I	−10416.93	N_{13}^+ I	−19352.31
N_4^+ D	−5948.07	N_{7a}^+ III	−10417.58	N_{14}^+ I	−20841.33
N_4^0 I	Not stable	N_{7b}^+ III	−10417.57	N_{14}^+ II	−20829.76
N_4^+ IV	−5943.51	N_8^+ I	−11905.66	N_{15}^+ I	−22330.65
N_4^0 IV	−5954.09	N_8^+ II	−11898.85	N_{16}^+ II	−23806.69
N_5^+ I	−7437.83	N_8^+ A	−11898.47	N_{18}^+ II	−26783.60
N_5^+ III	−7436.31	N_8^+ IV	−11906.00		

4.1.1. Series characteristics

Series I: The $n = 5$–15 members exhibit a "linear" chain-like structure. The bond distances are practically the same in all of the clusters, differing just in the second decimal place, the average being equal to 1.1 and to 1.3 Å for the terminal and internal N–N bonds, respectively. The angle between the terminal linear trimer segment and the internal dimer segment was found to be ~110° for all the structures. Moreover, an angle variation along the chain of 105–120° was observed. In particular, for the N_5^+ cluster, for which experimental results are available, we found the bond distances between the terminal and inner nitrogen atoms equal to 1.301 and 1.111 Å, in good agreement with the experiments and with the results of previous calculations [23]. The bond angles 112.6° (inner) and 166.1° (outer) are also in good agreement with the experiments (110.3° and 166.6°) [23]. The structures of the N_7^+, N_9^+ and N_{11}^+ clusters are very similar to those previously reported [17–19,22,23,26].

Series II: This series is characterized by *n*-even clusters formed by blocks of parallel N_2 units. All the members of this series exhibit a "zig-zag" like conformation, with almost equal angles in the lower and upper chains (106–108°). The N–N distance between any two internal atoms differs just in the second decimal place, the average value being equal to 1.5 Å, except for the bond between the terminal atoms of the upper and lower chains which averages to 1.2 Å.

Series III: This series is formed by the following stable members N_3^+ III, N_5^+ III, $N_{7a,b}^+$ III and N_9^+ III, and is characterized by the presence of a triangular N_3^+ core to which N_2 units are attached. The N_3^+ core is an equilateral triangle with sides of 1.316 Å. The distances from the N_2 units to the N_3^+ core, measured from the N atom of the N_2unit closest to the core, are equal to 2.407, 2.514, 2.504 and 2.56 (average) Å for $n = 5$, 7a, 7b and 9, respectively.

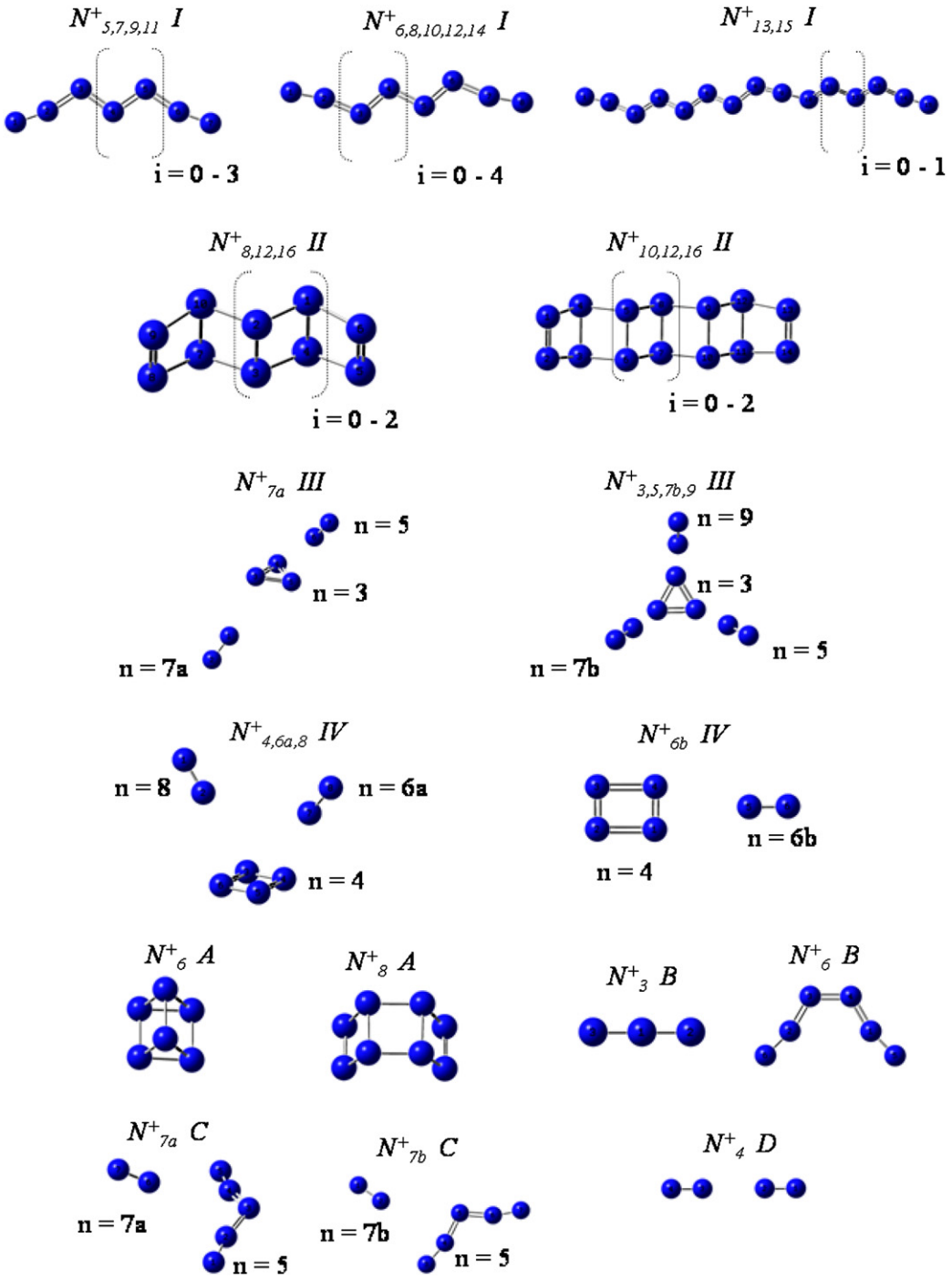

Fig. 1. Optimized geometries of the N_n^+ clusters at the B3LYP/6-311G** level of calculation.

Series IV: This series is formed by the members N_4^+ IV, $N_{6a,b}^+$ IV and N_8^+ IV and is characterized by the presence of a rectangular N_4^+, with sides of 1.199 and 1.625 Å, surrounded by N_2 units. The average distance from the N_2 units to the core, measured from the N atom of the N_2 unit closest to the core, is equal to 2.73 and 2.76 Å for $n = 6$ and 8, respectively.

At the present level of calculation, it is not possible to determine which of the $N_{7a,b}^+$ III and $N_{6a,b}^+$ IV isomers is the most stable.

4.1.2. A–D labeled clusters

Besides these clusters, four other sets of structures, labeled A, B, C and D in Fig. 1, have also been found:

– The structures labeled A are formed by interconnected N_2 units. The N_6^+ A structure is a equilateral triangular prism, with all sides and height in average equal to 1.5 Å, differing just in the second decimal place. The N_8^+ A species is similar to the N_8^+ II cluster, but exhibits a boat-like conformation. The N–N distance between

any two internal atoms of the clusters differs just in the second decimal place and averages to 1.5 Å, except that for the bond between the terminal atoms of the upper and lower chains which is in average equal to 1.2 Å.
- Structures labeled B can be viewed as formed by N_3 units (one and two). The N_3^+ B cluster is a linear trimer with bond distances equal to 1.18 Å, while the N_6^+ B is formed by two N_3 units connected by their terminal N atoms, in a boat-like conformation, with internal and terminal N–N bond distances equal to 1.12 and 1.31 Å, respectively.
- The structures labeled C derive from the cluster N_5^+ I by the attachment of one N_2 unit. The distance of the N_2 unit to the closest N atom of the N_5^+ I is equal to 3.00 and 3.04 Å for the N_{7a}^+ C and N_{7b}^+ C isomers, respectively.
- The structure labeled D is formed by two N_2 units, bonded by their terminal atoms in a linear conformation. The N–N distance is equal to 1.100 and 2.190 Å for the N_2 and the N_2–N_2 bond distance, respectively.

Although the clusters labeled A to D are apparently not structurally similar to those of Series I–IV, some of these species can be however related to those of the four series once an energy criterion is used to classify the clusters. This point will be discussed in the next section.

4.2. Deviation plot analysis (D-plot)

Let E_n^i, be the total energy of the ith isomer of the N_n^+ cluster (values in Table 1) and $E_{av}(n)$ the average energy of all n-isomers. The average energy shows a linear dependence on n: $E_{av}(n) = 10.13–1489.23n$ (Fig. 2a). For each isomer, the deviation energy D is defined as: $D_n = E_n^i – E_{av}(n)$, so that the smaller the D value, the lower the energy of the isomer and more stable it is.

From the D-plot (Fig. 2b) one sees that: (i) the cluster series can be characterized by their D behavior; (ii) for a given cluster size n, the D-plot shows the relative stability of the possible isomers and (iii) for a given series, the successive D value differences can be directly related to a commonly used stability function [30,31]. The Series I–IV, previously defined according to the criterion of conformational similarity, are also identified in the D-plot analysis (full lines in Fig. 2b). Furthermore, the D-plot analysis permits the identification of new series (dashed lines), revealing the connections between members of Series I–IV and the A–D labeled structures.

The structures labeled as A, B and C present almost the same positive slope of those of Series III and IV (Fig. 2b), which is probably related to the attachment of N_2 molecules (see Fig. 1) as the cluster size increases. Moreover, a negative slope in the D-plot characterizes changes from linear to triangular to rectangular structure of the cluster core as its size increases (e.g. the N_4^+ D → N_5^+ III → N_6^+ IVa,b).

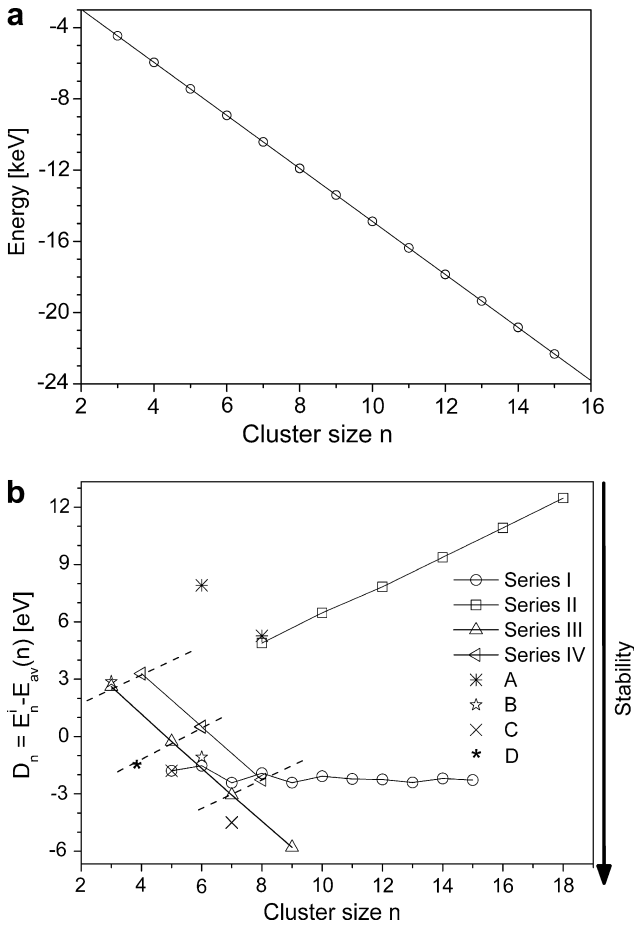

Fig. 2. (a) Total internal energy of the clusters as a function of the cluster size n. (b) D-plot: deviation of the internal cluster energy as a function of the cluster size n. The D-deviation is the difference of the average energy $E_{av}(n)$ and the cluster energy E_n^i.

4.3. Clusters stability and ionization potential effects on the mass spectra

The interpretation of mass spectral intensities is not straightforward and a proper description of the cluster formation requires a dynamical approach. Nevertheless, since the time scale of the TOF measurements is of the order of 10^{-6} s and that for reorganization and fragmentation through unimolecular processes is of the order of 10^{-14}–10^{-13} s [9], it is reasonable to assumed that the species being detected are the ones thermodynamically most stable. Based on this assumption, one would expect a correlation between the cluster population in the mass spectra and its stability.

4.3.1. Clusters stability and the mass spectrum abundances

Despite the systematical search performed, other N_n^+ structures may exist for a given n. However, it is reasonable to suppose that the main series are the ones already identified (Series I–IV). Within this assumption, the factors that affect the population in a mass spectrum are discussed.

The stability analysis shows that the members of Series I are more stable than those of the Series II (see Fig. 2). Within Series I, the stability analysis using the stability function S_n [30,31], defined as $S_n = E_{n-1} + E_{n+1} - 2E_n = D_{n-1} + D_{n+1} - 2D_n$, shows that the n-odd members are more stable than the n-even ones (Fig. 3). The tendency indicated by the stability analysis is, however, opposite to that of the mass spectra, where the n-even clusters are the most abundant ones (Fig. 4).

The mass abundance (or yield, Y) is a function of the production mechanism (P), the ionization mechanism (I) and the stability (S) of the clusters: $Y = F(P, I, S)$. Some insights on the cluster production and ionization mechanisms can be extracted from the fitting of the experimental population values, using the stability analysis results. We can assume that each series contributes exponentially to the mass spectra, since this behavior is characteristic of FF experiments [1,5,7,27]. Also, since the cluster mass varies almost linearly with its energy (see Fig. 2a), the desorption yields can expressed as

$$Y_n = \sum_i Y_i \ \exp\ \left(B_i E_n^i\right), \tag{1}$$

where Y_n is the experimental desorption yield of the N_n^+ ions, Y_i and B_i are the fitting parameters and E_n^i is the total energy of the cluster of size n of the ith series. In Eq. (1), the stability within the series (energy fluctuation) is explicitly taken into account ($S = S(E_n^i)$). Fig. 4 shows the results of the experimental desorption yields compared to the ones obtained from Eq. (1). According to the calculations, only clusters with $n > 9$, i.e. members of the Series I and II are stable and therefore contribute to the mass spectra. The experimental desorption yield description can be then reduced to

$$Y_n = Y_{\mathrm{I}} \ \exp\ \left(B_{\mathrm{I}} E_n^{\mathrm{I}}\right) + Y_{\mathrm{II}} \ \exp\ \left(B_{\mathrm{II}} E_n^{\mathrm{II}}\right) \tag{2}$$

The values of Y_n for $n = 16$, 17 and 18 are extrapolations of the fitting function, and a perfect agreement with the experiments is observed (Fig. 4). For $n < 9$ not enough data is available to perform the fitting according to Eq. (1).

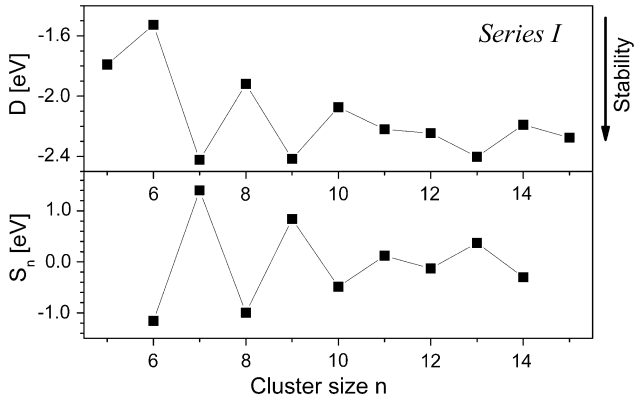

Fig. 3. The D-deviation (top) and stability (bottom) values for the members of Series I. Notice the higher stability of the n-odd clusters.

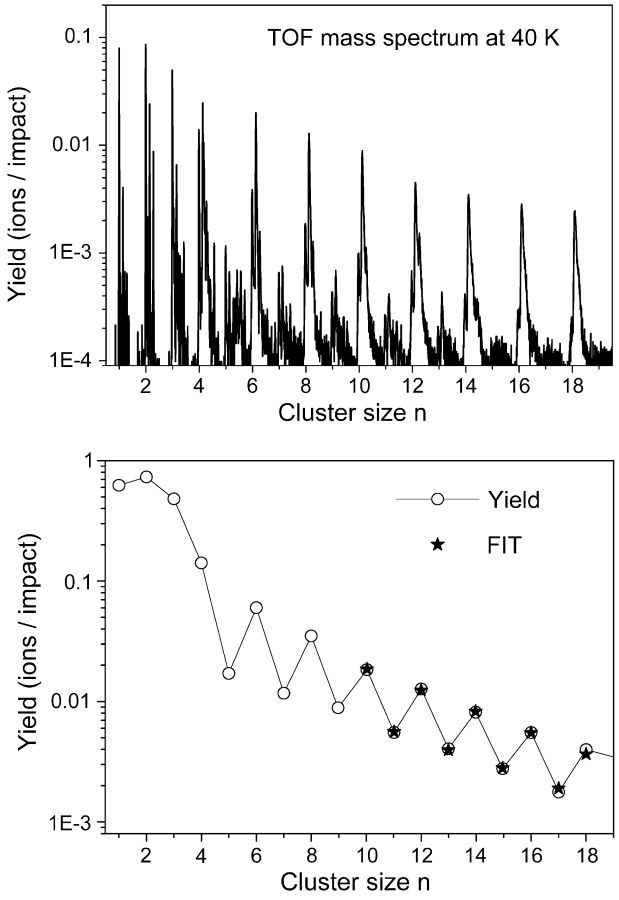

Fig. 4. TOF mass spectra (top) and total desorption yield (bottom, in semi-logarithmic plot) for the N_n^+ ion clusters produced by ^{252}Cf FF impact on the N_2 ice target. The values for $n = 16$–18 are extrapolation of the fitting function (as defined by Eq. (1)).

The fitting analysis gives very similar parameters for the contributions of the members of series I and II: $B_{\mathrm{I}} = 0.000116\ \mathrm{eV}^{-1}$ and $B_{\mathrm{II}} = 0.000136\ \mathrm{eV}^{-1}$. The desorption yield Y can then be expressed as a function of only one fitting parameter (within an error of less than 8%) characteristic of the desorption process $B = 0.000126 \pm 10^{-5}\ \mathrm{eV}^{-1}$ as

$$Y_n \cong \ \exp\ \left[BE_n^{\mathrm{I}}\right]\left\{Y_{\mathrm{I}} + Y_{\mathrm{II}} \ \exp\left[B\left(E_n^{\mathrm{II}} - E_n^{\mathrm{I}}\right)\right]\right\} \tag{3}$$

The fact that the experimental desorption yields can be fitted by using a unique fitting parameter (B) as a function of the cluster internal energy implies that the relative abundances, for $n > 9$, do not depend on the production and ionization mechanisms. The ratio $Y_{\mathrm{II}} \exp\left(B\left(E_n^{\mathrm{II}} - E_n^{\mathrm{I}}\right)\right)/Y_{\mathrm{I}}$ represents the relative abundances of Series I and II members. Since the fitting parameter B is very small as well as the energy difference between the isomers of the different series (a few eVs, as shown in the D-plot), the exponential factor is almost equal to one and the relative abundance is characterized by the $Y_{\mathrm{II}}/Y_{\mathrm{I}}$ ratio. The fact that the series II members are the most abundant is possibly related to the N_2 ice target characteristics, where the N_2 units are already pre-formed.

Table 2
Ionization potential (IP) of the four smallest nitrogen clusters calculated at the DFT/B3LYP/6-311G** level

Neutral → ion + e^-	Energy difference	IP (eV)*
$N^0 \rightarrow N^+ + e^-$	$E(N^+) - E(N^0)$	14.47 (14.53)
$N_2^0 \rightarrow N_2^+ + e^-$	$E(N_2^+) - E(N_2^0)$	15.84 (15.58)
N_3^0 VI → N_3^+ VI + e^-	$E(N_3^+$ VI$) - E(N_3^0$ VI$)$	12.57
N_3^0 III → N_3^+ III + e^-	$E(N_3^+$ III$) - E(N_3^0$ III$)$	10.76
N_4^0 IV → N_4^+ IV + e^-	$E(N_4^+$ IV$) - E(N_4^0$ IV$)$	10.58

* In parenthesis the experimental values of the ionization potential [29].

4.3.2. Ionization potential and the mass spectra abundances

The most abundant species in the mass spectra are the N_{1-4}^+ ions [7,8,11]. For ^{252}Cf FF [7] and 1.5 MeV/u Ar^{13+} [11] projectiles, the desorption yield of the N_2^+ ions is the highest, differently from the results obtained with electron or keV ion-impact desorption experiments, where the N^+ yield is the highest [8].

The first ionization potentials (IP) of the five smallest N_n^+ species are presented in Table 2. For $n = 3$, the two isomers, N_3^+ B and N_3^+ III, were considered; for $n = 4$, only the neutral rectangular isomer (relative to the N_4 IV structure) is stable. From Table 2 one sees that IP has its maximum value for $n = 2$ and decreases as n increases. On the other hand, the relative abundance of these ions ($n = 1$–4) do not follow their ionization potential tendency, since the IPs vary exactly in the opposite way to the abundances in the mass spectrum (Fig. 4). This result indicates that the abundance is related to the preferential emission of N_2 units in the ^{252}Cf FF electronic sputtering. The relative high desorption yield of the N_2^+ ions via a single process, probably due to a $(N_2)_n$-type of cluster formation, appears to be the reason for its larger yield.

4.3.3. The production mechanism and the mass spectra abundances

The analysis performed shows that, at least for $n > 9$, the ^{252}Cf FF abundances can be characterized by an exponential dependence of the clusters yield with its energy. On the other hand, since the ionization potentials are not directly related to the mass abundance, the production of the smaller clusters should involve a more complex mechanism.

Based on the large yields of N^+, N_2^+, N_3^+ and N_4^+ ions observed in the mass spectra, one order of magnitude higher than those of the larger species, it is reasonable to assume that two mechanism for the ionic cluster production are possible. The first production mechanism is related to the emission of species, hereafter called "pre-formed species", from the surface, induced by ion impact. This first production mechanism is responsible for the exponential decay observed for the clusters with $n > 3$. The second mechanism is responsible for the higher abundance of the smaller ions ($n = 1$–4), due to either (i) the condensation, into small clusters, of N and N^+ species that have been formed by atomization in the hottest region of the bombarded ice or (ii) the emission of "excited" pre-formed species (as a part of the first mechanism) that easily dissociate into smaller ions. The analysis performed in the previous sections cannot tell which one of the two processes is responsible for the ion cluster production. That is, the stability and the ionization potential analysis cannot distinguish if the larger clusters are formed by the combination of the four smallest clusters with neutral ones or if the larger clusters are initially formed and subsequently dissociated into those smaller ions. To accomplish that, a dynamical approach would be required.

These two mechanisms have been previously reported in [1], where the desorption yield of water cluster ions was studied for two types of projectiles: the ^{252}Cf FF ($E \sim 100$ MeV) and the N^+ ($E = 810$ keV). The exponential decay of the desorption yield with the cluster size, relative to the formation of pre-formed species, showed the same slope for both incident projectiles. However, only for the ^{252}Cf FF the second mechanism was observed, probably due to the larger energy deposited in the surface by the projectile.

5. Conclusions

Four series of nitrogen clusters, N_n^+, for $n = 2$–18 are identified in the systematical search performed at the DFT/B3LYP level of calculation. New members of the previously reported linear series have been found as well as three new series of clusters and some other stable structures. A new methodology is used to classify the different cluster structures based on the cluster internal energy, rather than its structure.

The experimental desorption yield was described as a function of the cluster internal energy using a unique exponential fitting parameter, characteristic of the ^{252}CF FF desorption process. For $n > 9$, the fact that the experimental desorption yields can be fitted, as a function of the cluster internal energy, using just one parameter (B), implies that their relative abundances do not depend on the production mechanisms. On the other hand, for the smaller clusters, the fact that the ionization potentials of the neutral clusters are not directly related to their parent ions mass abundance, suggests that a more complex production mechanism must be involved.

The stability and the ionization potential analysis cannot distinguish if the larger clusters are formed by the combination of the four smallest clusters with neutral ones or if the larger clusters are initially formed and subsequently dissociated into those smaller ions. To accomplish that, a dynamical approach is needed.

The relative high desorption yield of the N_2^+ ions via a single process and the high abundances of N_2 molecules (as pre-formed species) seems to be the reason of the larger yield of the even sized clusters.

Acknowledgements

The authors would like to acknowledge the Brazilian Agencies CNPq, Faperj and CLAF for their support.

References

[1] V.M. Collado, L.S. Farenzena, C.R. Ponciano, E.F. da Silveira, K. Wien, Surf. Sci. 569 (2004) 149.
[2] L.S. Farenzena, V.M. Collado, C.R. Ponciano, E.F. da Silveira, K. Wien, Int. J. Mass Spectrom. Ion Proc. 243 (2005) 85.
[3] C.R. Ponciano, L.S. Farenzena, V.M. Collado, E.F. da Silveira, K. Wien, Int. J. Mass Spectrom. Ion Proc. 244 (2005) 41.
[4] L.S. Farenzena, R. Martinez, P. Iza, C.R. Ponciano, M.G.P. Homem, A. Naves de Brito, E.F. da Silveira, K. Wien, Int. J. Mass Spectrom. 255 (2006) 1.
[5] R. Martinez, C.R. Ponciano, L.S. Farenzena, P. Iza, M.G.P. Homem, A. Naves de Brito, K. Wien, E.F. da Silveira, Int. J. Mass Spectrom. 253 (2006) 112.
[6] C.R. Ponciano, R. Martinez, L.S. Farenzena, P. Iza, M.G.P. Homem, A. Naves de Brito, E.F. da Silveira, K. Wien, J. Am. Soc. Mass Spectrom. 17 (2006) 1120.
[7] L.S. Farenzena, P. Iza, R. Martinez, F.A. Fernandez-Lima, E.D. Seperuelo, G.S. Faraudo, C.R. Ponciano, M.G.P. Homem, A. Naves de Brito, K. Wien, E.F. da Silveira, Earth Moon Planets 97 (2005) 311.
[8] Y. Baba, T. Sekiguchi, I. Shimoyama, Surf. Sci. 593 (2005) 324.
[9] R.E. Johnson, Energetic Charged Particle Interactions with Atmospheres and Surfaces, Springer Verlag, Heidelberg, 1990.
[10] D.E. Woon, Icarus 149 (2001) 277.
[11] T. Tonuma, H. Kumagai, T. Matsuo, H. Shibata, H. Tawara, Int. J. Mass. Spectrom. Ion Proc. 135 (1994) 129.
[12] R.D. Lorenz, J.I. Lunine, Icarus 122 (1996) 79.
[13] W.J. Lauderdale, J.F. Stanton, R.J. Barlett, J. Phys. Chem. 96 (1992) 1173;
S.C. de Castro, H.F. Schaeffer III, J. Chem. Phys. 74 (1981) 550.
[14] Q.S. Li, X. Hu, W. Xu, Chem. Phys. Lett. 287 (1998) 94.
[15] X. Wang, Y. Ren, M.B. Shuai, N.B. Wong, W.K. Li, A.M. Tian, J. Mol. Struct.: Theochem 538 (2001) 145.
[16] L. Gagliardi, S. Evangelisti, B.O. Roos, P. Widmark, J. Mol. Struct.: Theochem 428 (1998) 1.
[17] Y.D. Liu, P.G. Yiu, J. Guan, Q.S. Li, J. Mol. Struct.: Theochem 588 (2002) 37.
[18] S. Evangelisti, T. Leininger, J. Mol. Struct.: Theochem 621 (2003) 43.
[19] D.A. Dixon, D. Feller, K.O. Christe, W.W. Wilson, A. Vij, V. Vij, H.D.B. Jenkins, R.M. Olson, M.S. Gordon, J. Am. Chem. Soc. 126 (2004) 834.
[20] H. Zhou, W. Zheng, X. Wang, Y. Ren, N. Wong, Y. Shu, A. Tian, J. Mol. Struct.: Theochem 732 (2005) 139.
[21] J. Gu, K. Chen, H. Jiang, J. Chen, R. Ji, Y. Ren, A. Tian, J. Mol. Struct.: Theochem 428 (1998) 183.
[22] C.K. Law, W.K. Li, X. Wang, A. Tian, N.B. Wong, J. Mol. Struct.: Theochem 617 (2002) 121.
[23] L. Gagliardi, G. Orlandi, S. Evangelisti, B.O. Roos, J. Chem. Phys. 114 (24) (2001) 10733.
[24] T.J. Lee, J.E. Rice, J. Chem. Phys. 94 (2) (1991) 1215.
[25] F.J. Owens, J. Mol. Struct.: Theochem 623 (2003) 197.
[26] W. Xu, G. Li, L. Wang, S. Li, Q. Li, Chem. Phys. Lett. 314 (1999) 300.
[27] K. Wien, C.S.C. de Castro, Nucl. Instrum. Meth. B 146 (1998) 178.
[28] Jaguar 5.5 and Jaguar 6.0, Schroedinger Inc. Portland, Oregon, 2004.
[29] Handbook of Chemistry and Physics, ed. D.R. Lide, CRC Press, Inc. 1995.
[30] F.A. Fernandez-Lima, C.R. Ponciano, E.F. da Silveira, M.A. Chaer Nascimento, Chem. Phys. Lett. 426 (2006) 351.
[31] F.A. Fernandez-Lima, C.R. Ponciano, M.A. Chaer Nascimento, E.F. da Silveira, J. Phys. Chem. A 110 (2006) 10018.